Journal of the European Ceramic Society 22 (2002) 199–207

www.elsevier.com/locate/jeurceramsoc

Quantitative characterization of various tetragonal zirconia polycrystals (TZPs)

C.-C.T. Yang, H.J. Cho, W.J. Wei*

Institute of Materials Science and Engineering, National Taiwan University, 1 Roosevelt Road, Section 4, Taipei, Taiwan 106, ROC

Received 12 October 2000; received in revised form 8 March 2001; accepted 24 March 2001

Abstract

The microstructures, Y_2O_3 content and phases of 3 mol% yttria-doped tetragonal zirconia polycrystals (TZPs) were quantitatively investigated. Five yttria-doped zirconia samples were observed by scanning electron microscopy (SEM) equipped with energy dispersive spectroscopy (EDS) or electron probe microanalyzer (EPMA) equipped with wavelength dispersive spectroscopy (WDS). The amount of phase transformation was determined by X-ray diffractometry (XRD). Operating conditions of EDS or WDS were controlled based on the needs of statistical analysis. The Student's t distribution in a confident interval of 99% was adopted and applied to reveal the level of homogeneity of Y_2O_3 content in five TZP samples. Based on the results and analytical methods, the quality, including sintered density, the fraction of large grains, the transformation capability, and the homogeneity of Y_2O_3 content of TZP can be distinctly verified.

Keywords: Dopant distribution; Homogeneity; Microsturcture-final; TZP; Y_2O_3; ZrO_2

1. Introduction

Zirconia has widely attracted attention because of phase transformation toughening phenomena.[1–3] Its unique features such as high strength, high toughness, chemical stability, high melting temperature, ionic, electrical and optical properties make the zirconia a promising engineering material. The applications of zirconia include wear-resistant components, solid state electrolyte, and gemstone, etc. Pure zirconia material has been of limited use as advanced structural ceramics due to its spontaneous tetragonal to monoclinic phase transformation when cooled to room temperature from fabrication temperature, causing about 4.5% volume expansion and thus catastrophic fracture.

In order to overcome this problem, a series of phase stabilizers are added to retain the high temperature cubic or tetragonal phase. These typical stabilizers include calcia, magnesia, yttria, ceria and other rare earth oxides. The zirconia materials fabricated by adding phase stabilizers contain highly metastable tetragonal (t-ZrO_2) phases, which may transform to monoclinic phase as the stress intensity is greater than a critical value. In the vicinity of a crack the metastable t-phase grains transform, resulting in a volume increase; therefore, the crack propagation is retarded by the compressive stress caused by the transformation. This phenomenon is so-called phase transformation toughening and it helps improve the fracture behavior of zirconia materials.

According to the microstructures obtained by using different heat treatments and stabilizer content, zirconia materials can be divided into three basic types, including fully stabilized zirconia (FSZ), partially stabilized zirconia (PSZ), and tetragonal zirconia polycrystal (TZP). TZP has better mechanical properties than PSZ due to small grain size and better grain boundary coherency. It is reported[4,5] that the amount of Y_2O_3 affects the grain size, the Martensitic phase transformation temperature, strength and degradation behavior of TZP, especially in humid environment. In this research, five different sources of 3Y-TZP powders were compared to provide the basis for choosing the better powder. Therefore, a fully quantitative analysis of Y_2O_3 was made to realize the spatial and quantitative variation of Y_2O_3 content. Besides, the average grain size, the fraction of large grains, the transformed phases were quantified in order to compare the relationship of the distribution of Y_2O_3 content.

* Corresponding author. Tel.: +886-2263-023, ext. 2701; fax: +886-22363-4562.

E-mail address: wjwe@ccms.ntu.edu.tw (W.J. Wei).

0955-2219/01/$ - see front matter
PII: S0955-2219(01)00261-8

2. Experimental procedures

Colloidal processing developed by previous work[6] was adopted to fabricate four testing samples, including TZYS (Tosoh, Japan), HSY-3.0 (Daiichi, Japan), HWAZY3P (Hanwha, Australia) and CH9910-Y (NTHU, Mainland China). These four ZrO_2 slurries were prepared based on 28 vol.% solid loading, milled for 24 h and then casted at a gas pressure of 10 kg/cm^2. The fifth sample PL-D was die-pressed due to the high surface area of the powder, which was non-dispersive. Five different Y-TZP green bodies were sintered at 1480°C for 1 h.

The green and sintered densities of five samples were measured by Archimedes' method. The mean grain size of the samples was determined from the SEM micrographs by linear intercept technique.[7] More than 200 grains were counted on the micrographs. For those grains which are larger than 1 μm[1] are defined as big grains. The quantitative analyses of yttria content in various zirconia samples were determined either by a SEM (XL30, Philips Co., The Netherlands) equipped with EDS (DX-4, EDAX Co., USA) or an EPMA (JXA-8600SX, Jeol Co., Japan) equipped with WDS. A sintered Tosoh TZYS was used as the standard specimen which contains 5.07 mass% Y_2O_3, corresponding to 2.83 mol%. The operating conditions such as magnification (2000×), spot size (60 μm), probe current (1×10^{-7}A), working distance (10 mm), tilting angle (15°) and take-off angle (45.3°) of two microscopes were all kept constant. The detailed calibration procedures used for quantitative analysis were referred to a user's manual for EDS[8] and EPMA.[9]

These five samples were ground against 800 mesh metal-bonded diamond wheel so as to test the transformability. The speed of the wheel was 2400 rpm and the table speed of the surface grinder was 2.1 m/min. The ground samples were then annealed at 1200°C without soaking and cooled to room temperature both at a ramp of 10°C/min. The change of t-to-m phase content of Y-TZP samples either ground or annealed was quantitatively determined by an X-ray diffractometer (XRD, PW 1710, Philips Instrument, The Netherlands) using Cu K_α radiation according to the procedures given by Toraya et al.[10] and Garvie et al.[11]

3. Statistical analysis of spectroscopic study

3.1. Description of background measurement

In order to obtain a better microstructural image, the samples were gold coated because the atomic number of gold was higher, causing higher secondary electron intensity. However, for quantitative analyses of Y_2O_3 content, it is necessary to deposit carbon instead of gold to avoid the overlapping of Au and Zr spectra when analyzed by using SEM equipped with EDS. Due to the overlapping of Zr L_α and Y L_α, the higher accelerated voltage of electron beam was chosen and the Zr K_α and Y K_α was used as the basis of quantitative measurement. Moreover, for quantitative analyses of Y_2O_3 content determined by using EPMA equipped with WDS, the energy spectra of Zr L_α and Y L_α can be resolved, therefore the first strongest peak of Zr and Y was used as the basis of quantitative measurement. Besides, the thickness of the samples was kept the same so as to obtain higher accuracy of Y_2O_3 content measurement.

3.2. Consideration of X-ray counts

It is well known that the X-ray production is statistical in nature. As the electron beams bombard the sample, the X-rays are generated and interact with the EDS or WDS detectors. One can find that the intensity of X-ray is completely random but has a fixed mean value, also called arithmetic mean. The relationship between the distribution of X-ray counts and the integrated intensity of X-ray in a given time may be expressed and approximated by a continuous normal/Gaussian distribution. Let us designate the mean number of X-ray counts produced for a given sample as $\overline{N}$ and standard deviation of the X-ray intensity measurement as S_c. The standard deviation of the intensity measurement for small sampling ($n < 30$) is defined as:[12–15]

$$S_c = \left[\sum_{i=1}^{n} \frac{(N_i - \overline{N})^2}{n-1}\right]^{1/2} \quad (1)$$

Also the mean value of the number of X-ray counts can be calculated and expressed as:

$$\overline{N} = \frac{\sum_{i=1}^{n} N_i}{n} \quad (2)$$

Yakowitz et al.[16] proposed a simplified criterion for the homogeneity of a second component. If all of the data points fall within the $\overline{N} \pm 3\overline{N}^{1/2}$ limits, then the phase or the sample is said to be homogeneous. The variation of the component or element of interest in the sample represents the level of homogeneity and is expressed as:

$$\mathrm{Var}(\overline{N}) = \frac{\pm 3\overline{N}^{1/2}}{\overline{N}} \quad (3)$$

Usually, a level of homogeneity of $\leqslant \pm 1.0\%$ is desired and therefore 90,000 X-ray counts have to be accumulated. In other words, the total counting time of 50–100 s is necessary for precise measurement of Y_2O_3

[1] All reported grain sizes in this study have been corrected with a factor, 1.56.

content in ZrO_2 matrix if the detected rate of X-ray spectra is in the range of 2000–3000 counts per second.

3.3. Confidence of small sampling

Goldstein et al.[17] proposed a more exact determination of the range (wt.%) and level (%) of homogeneity of the element of interest in sample. That involves the use of the standard deviation (S_c) of the measured values, and the degree of statistical confidence in the determination of $\overline{N}$. Therefore, the level of homogeneity for a given confident coefficient, $1-\alpha$, is given by

$$\pm\frac{W_{1-\alpha}}{C}=\pm\left(\frac{t_{n-1}^{\alpha/2}}{n^{1/2}}\right)\frac{S_c}{\overline{N}} \tag{4}$$

where C is the true mass fraction of the element of interest, n is the number of measurements, and $t_{n-1}^{\alpha/2}$ is the Student's t distribution for a $\alpha/2$ confident coefficient and for $n-1$ degrees of freedom. The probability (P) of random sampling points to be outside the confident level is expressed as:

$$P\left(-t_{n-1}^{\alpha/2}<t<t_{n-1}^{\alpha/2}\right)=1-\alpha \tag{5}$$

The $1-\alpha$ confident level for population mean (μ) on the basis of a sample mean ($\overline{X}$) for small sampling is given by:

$$\overline{X}-t_{n-1}^{\alpha/2}\frac{S}{n^{1/2}}<\mu<\overline{X}+t_{n-1}^{\alpha/2}\frac{S}{n^{1/2}} \tag{6}$$

It has been shown[12,14] that if the number of measurement is less than 4, the value of Student's t distribution, $t_{n-1}^{\alpha/2}$ will deviate largely from the real situation. In other words, under the things being equal the confident coefficient will become too low. Therefore, the number of measurement of Y_2O_3 content for small sample ($n<30$) is suggested to be at least 4 during the quantitative analysis.

4. Results and discussion

4.1. Densification

The physical properties of five ZrO_2 powders are listed in Table 1. These Y-TZP powders were formed through the colloidal processing except for sample PL-D. The green density and sintered density are listed in Table 2. The Tosoh TZYS samples have the highest green and sintered density, corresponding to 56.4 and 99.8% theoretical density (T.D.), respectively. The densities of other samples are expressed in sequence from higher to lower value: i.e. Daiichi HSY-3.0 (99.1% T.D.), HWA–ZY3P (98.5% T.D.), CH9910-Y (98.5% T.D.) and PL-D (95.9% T.D.). It is doubted that the adopted die-pressing process may cause the lower density of PL-D sample. However, our previous results[6,18] show the density variation of Tosoh TZYS sample either formed by colloidal processing or die pressing is $\pm0.2\%$ if sintered above l480°C/1 h, Therefore, it is concluded that the density of PL-D sample is inferior to others mentioned above in spite of different shape-forming method.

4.2. Microstructures

The microstructures of five different sintered bodies are shown in Figs. 1–3. In order to have a precise grain size measurement, the thermal etching condition among five samples is a little different. For Tosoh TZYS and PL-D samples, the etching conditions are 1280°C for 15 mm while the others are 1280°C for 20 min.

Fig. 1 shows the microstructures of Tosoh TZYS sample. It has a sintered density of 99.8% and a mean

Table 1
The physical properties and purity of ZrO_2 powders used in this research

Properties	Source				
	Tosoh[a] TZYS (Tosoh, Japan)	Daiichi[a] HSY-3.0 (Daiichi, Japan)	PL-D[b] (Russia)	HWA-ZY3P[a] (Hanwha, Australia)	CH9910-Y[b] (Mainland China)
Specific surface area (m^2/g)	15.7	4–10	NA[c]	14	NA
Particle size, d_{50} (μm)	0.3	0.4–0.7	NA	0.4	NA
Composition (mass%)					
Y_2O_3	5.07	5.40	5.13	5.2	5.40
Al_2O_3	<0.005	0.25	0.24	0.02	0.25
SiO_2	<0.002	0.15	0.00	0.04	0.00
Fe_2O_3	<0.002	<0.01	1.24	0.03	<0.01
Na_2O	0.023	0.03	0.14		0.06

[a] Data sheet supplied by vendors.
[b] Supplied and measured by ICP in NTU.
[c] Not available.

Table 2
The densities, average grain size, and the fraction of big grain of different sintered TZPs

	Tosoh TZYS	Daiichi HSY-3.0	HWA-ZY3P	CH9910-Y[a]	PL-D[b]
Green density (g/cm^3)	3.40 (56.4% T.D.)[c]	3.15 (52.2% T.D.)	3.11 (51.6% T.D.)	2.58 42.8% T.D.)	2.38 (40.9% T.D.)
Sintered density (g/cm^3)	6.02 (99.8% T.D.)	5.98 (99.1% T.D.)	5.94 (98.5% T.D.)	5.94 (98.5% T.D.)	5.78 (95.9% T.D.)
Average grain size (μm)	0.41	0.40	0.47	0.40	0.45
Big grain[d] (%)	<0.1	1.2	1.5	3.5	2.9

[a] Prepared slurry with 20 vol.% solid loading.
[b] Prepared by die-pressing.
[c] Theoretical density (T.D.) = 6.03 g/cm^3.
[d] The grain size is larger than 1 μm.

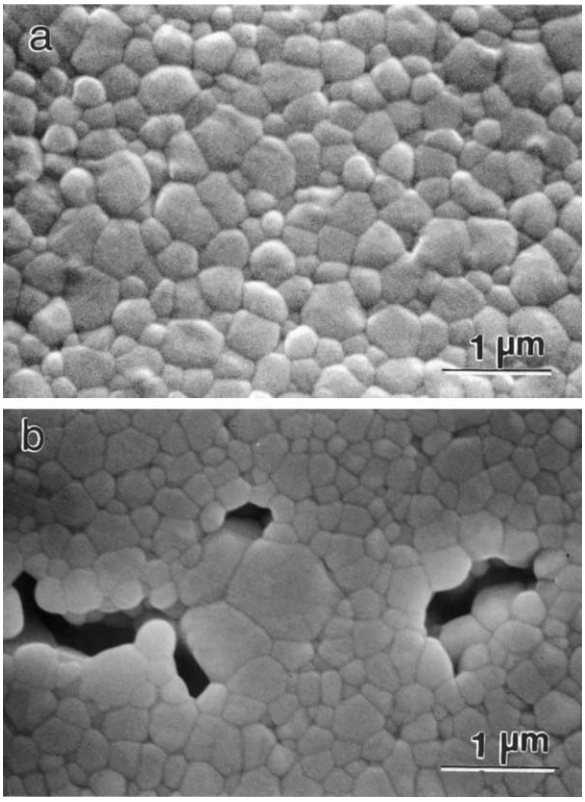

Fig. 1. SEM micrographs of (a) thermal-etched Tosoh TZYS, (b) the remanent hole after sintering. The average grain size is 0.41 μm. Thermal etching conditions for the sample were 1280°C for 15 min.

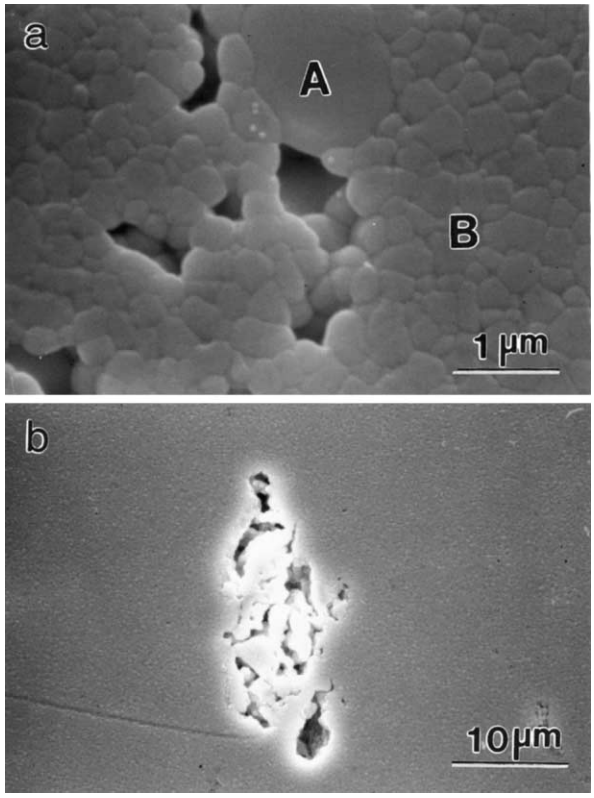

Fig. 2. SEM micrographs of thermal-etched PL-D (a) big grain and (b) hard agglomerate. The average grain size is 0.45 μm. The thermal etching conditions for the sample were 1280°C for 15 min.

grain size of 0.41 μm. Occasionally, the residual pores in range of 1–3 μm caused by hard agglomerates were found and might be responsible for fracture origins. Similar residual pores due to a poor inherent property of hard agglomeration can be found in the other four samples. Fig. 2 shows typical large grains and hard agglomerate found in PL-D sample. Moreover, the large grains, which are defined as larger than 1 μm, are easily found in the vicinity of residual pores, as shown in Fig. 2(a). The amount of large grains is about 2.9 vol.% and may have relation to the content of Y_2O_3 in the grains.

The grain size and amount of large grains of the other samples are listed in Table 2. The grain size of Daiichi HSY-3.0 and CH9910-Y is the smallest (0.40 μm), shown in Fig. 3(a) and (b). The density of Daiichi HSY-3.0 and CH9910-Y is a little lower than that of Tosoh TZYS, but has almost the same grain size. The grain size of HWA-ZY3P is in the range of 0.47 μm, as shown in Fig. 3(c).

The Tosoh TZYS sintered sample which contains an average Y_2O_3 content of 5.07 mass% Y_2O_3, corresponding to 2.83 mol% was used as the base of comparison. The amount of Y_2O_3 content, mean value $(\overline{X})$,

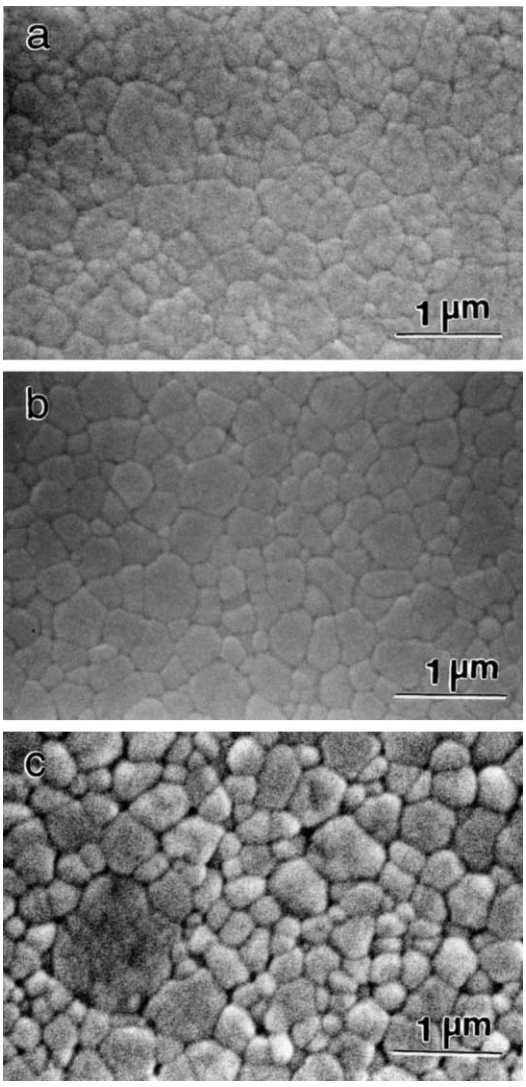

Fig. 3. SEM microstructure of(a) Daiichi HSY-3.0, (b) CH9910-Y and (c) HWA-ZY3P. The average grain sizes for Daiichi HSY-3.0, CH9910-Y and HWA-ZY3P are 0.40, 0.40 and 0.47 μm, respectively. The thermal etching conditions for the samples were 1280°C for 20 min.

standard deviation (S), level of homogeneity ($\pm W_{1-\alpha}/C$) and confident interval ($l < \mu < u$, where l and u stand for lower and upper limits of confident level of 99%) of five different Y-TZP samples determined by EDS are listed in Table 3. it is found that Daiichi HSY-3.0 has an average of 5.34 mass% (2.99 mol%) and is the highest among these TZP samples. Sample PL-D shows the lowest amount of Y_2O_3 and has an average of 4.92 mass%. The distribution of Y_2O_3 content for Tosoh TZYS, Daiichi HSY-3.0 and HWA-ZY3P is good compared to that of PL-D and CH99 1 0-Y.

Due to the lower intensity of K_α in EDS spectra, it may lead to higher error when using the intensity of K_α as the measurement basis. For the measurement of Y_2O_3 content by EPMA, the spectrum of Zr L_α and Y L_α can be separated in the WDS, therefore the L_α peaks of Zr and Y which show a higher intensity were also examined. The EPMA results are also shown in Table 3. The Y_2O_3 content of these five TZPs samples is close to that measured by EDS.

The level of homogeneity of Y_2O_3 content and confident interval for these five TZPs samples calculated according to Eqs. (4) and (6) are listed in Table 3. The results show that the level of homogeneity of Y_2O_3 content for CH9910-Y and PL-D is 12.3 and 5.58%, respectively, implying the level of homogeneity is quite poor compared to the other three TZPs when analyzed by SEM-EDS. Even though the level of homogeneity of Y_2O_3 content for CH9910-Y and PL-D is inferior to the three samples, all of the sampling data points are still in the range of confident interval.

When analyzing by EPMA, one can find samples Daiichi HSY-3.0 and CH9910-Y have a higher amount of Y_2O_3 content when compared to the other three TZP samples. Moreover, the EPMA results show that sample Tosoh TZYS has the best level of homogeneity of Y_2O_3 content. The level of homogeneity of the other four TZPs samples is from 5.37 to 8.81%, and relatively poor compared to the sample Tosoh TZYS.

After the measurement of Y_2O_3 content quantified either by EDS or WDS, one can find the best level of homogeneity of Y_2O_3 in five ZrO_2 matrix is in the following sequence: Tosoh TZYS, Daiichi HSY-3.0, HWA-ZY3P, PL-D and CH9910-Y for EDS results; Tosoh TZYS, Daiichi HSY-3.0, HWA-ZY3P, CH9910-Y and PL-D for WDS results. It can be found that samples Tosoh TZYS, Daiichi HSY-3.0 and HWA-ZY3P have similar level of homogeneity of Y_2O_3 content while samples PL-D and CR9910-Y show a relatively poor distribution of Y_2O_3 content. The above results have shown that both two techniques provide reliable data. However, WDS measurement is a time-consuming task due to longer collection time compared with EDS. The latter technique is a more convenient tool for the estimation of the homogeneity of Y_2O_3 content in ZrO_2 matrix.

Besides, the amount of big grains of Y_2O_3 content is also plotted in Fig. 4. The evidence appears that sample Tosoh TZYS, which shows the best level of homogeneity of Y_2O_3 content also has the least amount of big grains while samples PL-D and CH9910-Y, showing a relatively poorer level of homogeneity of Y_2O_3 content have higher probability of finding big grains. Lange[4,19] reported that the density of zirconia sintered bodies and the amount of Y_2O_3 content affects the crystalline phase and grain size of zirconia sintered bodies. The dense the matrix, the higher the amount of tetragonal phase. Because the density of sintered body is higher, a confined force makes grains more difficult for the spontaneous transformation of t-to-m phase during the cooling step from sintering temperature.

Table 3
Quantitative results of the Y_2O_3 content in TZP analyzed by SEM-EDS or EPMA

Sample	EDS*[a]					EPMA**[a]				
	Y_2O_3 content (mass%)	$\overline{X}$ (mass%)	S (mass%)	$\pm\frac{W_{1-\alpha}}{C}$ (%)	$l<\mu<u$ (mass%)	Y_2O_3 content (mass%)	$\overline{X}$ (mass%)	S (mass%)	$\pm\frac{W_{1-\alpha}}{C}$ (%)	$l<\mu<u$ (mass%)
Tosoh TZYS	5.07 5.08 5.17 5.11	5.11	0.045	2.57	4.98–5.24	5.054 4.983 5.102 5.072	5.05	0.051	2.95	4.90–5.20
Daiichi HSY-3.0	5.31 5.38 5.29 5.39	5.34	0.049	2.68	5.20–5.48	5.425 5.495 5.353 5.263	5.38	0.099	5.37	5.09–5.67
CH9910-Y	5.21 5.09 5.56 5.49	5.33	0.224	12.3	4.68–5.98	5.345 5.190 5.482 5.525	5.39	0.152	8.24	4.95–5.83
HWA-ZY3P	5.00 5.08 4.96 4.99	5.01	0.051	2.97	4.86–5.16	4.887 5.088 4.950 5.071	5.00	0.097	5.67	4.72–5.28
PL-D	4.83 4.90 4.89 5.05	4.92	0.094	5.58	4.65–5.19	5.007 4.792 4.846 5.118	4.94	0.149	8.81	4.50–5.38

[a] Test conditions. *Mag. 2000×; working distance = 10 mm; take-off angle = 45.3°, ZrO_2 CPS = 2400–2700; Y_2O_3 CPS = 180–200. **Mag 2000×; ZrO_2 CPS = 7300–7400; Y_2O_3 CPS = 370–410.

It is believed[4,19] that the variation of Y_2O_3 content in matrix may locally affect pore formation and exaggerate the grain growth. The large grains in the vicinity of residual pores can be found easily, as shown in Figs. 1(b) and 2(a). The situation is the worst in the case of PL-D sample. It is suspected that the Y_2O_3 content in this area may be different from other areas. The analysis by EDS reveals that the Y_2O_3 content is 3.99 mass% and significantly lower than the average value of 4.92 mass%. Besides, the measurement is also done by EPMA on the large grain indicated as marks A and B, as shown in Fig. 2(a). The amount of Y_2O_3 content is 4.67 mass% in A region (a large grain) and 5.21 mass% in B region (matrix grains), it is speculated that the formation of large grains has the relation to the lower Y_2O_3 content. The result is consistent with the literature reported by Lange[4] who proposed the size of tetragonal phase can be controlled by cubic phase. He reported that the grain size was governed by Y_2O_3 content. ZrO_2 with 1.5–4.5 mol% Y_2O_3 content that falls in the t + c phase region has the smallest grain size. Analyses of selected area electron diffraction have shown that the larger grains distributed among the smaller grains have the cubic structure, whereas the smaller grains are tetragonal. But based on our observation, it is hard to make conclusive remark on the relationship between the amount of cubic grains and the growth of tetragonal grains.

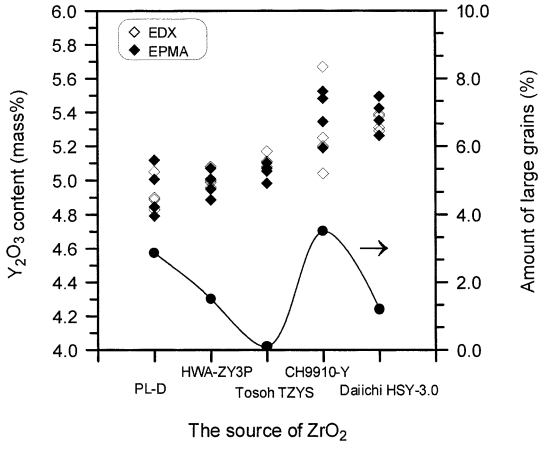

Fig. 4. The Y_2O_3 content and amount of big grains of different TZPs analyzed by SEM-EDS or EPMA.

Moreover, it is possible that the exaggerated grain growth may be due to the difference in local packing densities of these five TZP samples. However, Tosoh TZYS, Daiichi HSY-3.0, HWA-ZY3P, and CH9910-Y were formed by colloidal processing under the same pressure casting conditions, but had different green densities. Therefore, it may be concluded that powder properties such as particle size and shape, etc., as indicated in Table 1, may play an important role in the formation of large grains. Under these variables being

nearly equal, the poor distribution of Y_2O_3 content may be the major reasons responsible for the abnormal grain growth.

From the statistical review, it is suggested that the minimum measurement number for quantitative analysis should be at least 4. Otherwise, it may cause errors during small sampling. Of course, the probability of measuring Y-content just using 4 microprobe analyses is rather small. As indicated in Table 2, the percentage of large grains found in these five TZPs samples is from 0.1 to 3.5%. Our results show that the large grains have relation with the level of homogeneity of Y_2O_3 content. Therefore, the elemental analysis on the specific grains and this technique can be used for what it is intended for.

Furthermore, Fig. 5 shows the statistics of Y_2O_3 content of sample Daiichi HSY-3.0 in ZrO_2 matrix. The results of 30 measurements show the Y_2O_3 content is in the range of 4.63–5.47 mass%. The average Y_2O_3 content is 5.11 mass% which is lower than that for small sampling ($n=4$). The result shows that the probability of finding inhomogeneous distribution of Y_2O_3 content also increases as the sampling number increases. The Y_2O_3 content can be as low as 4.63 mass%. As it shows, the distribution of Y_2O_3 content tends toward Gaussian distribution as the testing number is larger than 30.

4.3. The effect of machining on crystallinity and microstructure

The crystallinity changes due to t-to-m phase transformation during the surface grinding.[20] Therefore, the amount of monoclinic phase of four as-sintered, ground and annealed Y-TZP samples was determined by Q-XRD. Fig. 6 shows the spectra illustrating the changes of TZYS in crystallinity in various stages. The amount of m-phase of as-sintered samples (X_m) is almost 0%. In other words, the as-sintered samples consist of 100% tetragonal phase. But the amount of m-phase of the ground samples is 2.6%. In additional to t-to-m phase transformation, the asymmetrical broadening phenomena of t-phase (111) plane is also observed. This is due to the formation of r-phase.[21,22] The angle of $(111)_r$ ($2\theta = 29.57°$) and $(111)_t$($2\theta = 30.17°$) are pretty close. After thermal annealing at 1200°C for 0 h, the amount of m-phase decreases to 0% and the asymmetrical broadening effect is also eliminated.

Moreover, the surface treatment also affects the ratio of I_{002}/I_{200} The ratio of I_{002}/I_{200} of the as-sintered samples is 0.74 and increases to 1.69 and 2.34 for ground samples and annealed samples, respectively. The changes in the ratio of I_{002}/I_{200} is caused by the domain reorientation. Lankford et al.[23] proposed that as grains were under compressive stress, the domains of c-axis parallel to stress axis re-orientated, making the neighboring domain boundaries move toward the reverse direction. That makes the domains of the c-axis parallel to stress axis disappear. At the same time, the grains along [010] direction or [100] direction elongate slightly. This is so-called ferroelastic domain switching phenomena.[24]

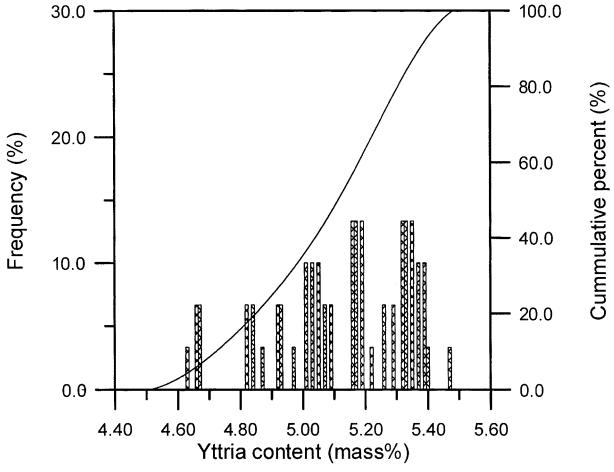

Fig. 5. The distribution of Y_2O_3 content of sample Daiichi HSY-3.0 in ZrO_2 matrix. The Y_2O_3 content is in the range of 4.63–5.47 mass%. As central limit theorem states the distribution of Y_2O_3 content tends toward the Gaussian distribution as the measurement number is larger than 30.

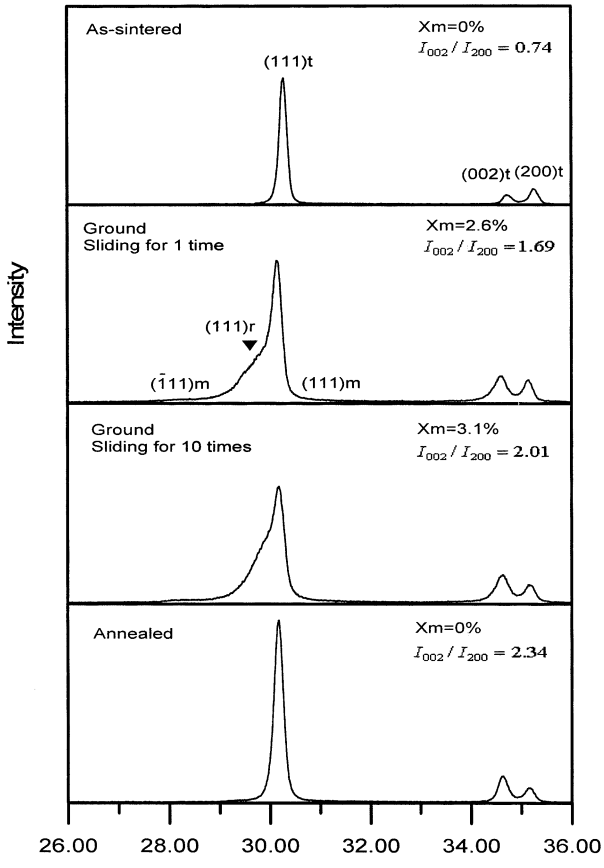

Fig. 6. The phase change of as-sintered, ground, and annealed Tosoh TZYS dense samples.

Besides Tosoh TZYS, the other three Y-TZP samples have the same phenomena. The amount of m-phase of ground and annealed samples is summarized in Table 4. Among four Y-TZP samples, Daiichi HSY-3.0 has the maximum amount of m-phase (3.8%) while Tosoh TZYS has the minimum as ground by specified conditions. The amount of m-phase of all samples decreases to 0% after the annealing treatment.

In addition to m-phase occurrence and peak broadening, the machining also affects the microstructure. The ground morphology of ground Tosoh TZYS after heat treatment (1200°C/0h) is shown in Fig. 7, illustrating a refinement of grains after annealing. The grain size decreases from 0.41 μm to 0.20 μm. The grain size refinement may improve the low temperature degradation behavior of Y-TZP.[21] Among the Y-TZP samples, Daiichi HSY-3.0 has the smallest grain size (0.17 μm) after the annealing treatment.

Table 4
The t-phase change and average grain size of as-sintered, ground, and annealed of different TZPs

m-Phase content	Tosoh TZYS	Daiichi HSY-3.0	HWA-ZY3P	CH9910-Y
As-sintered	0%	0%	0%	0%
Ground — 5 μm/pass	2.6	3.1	2.7	3.0
Ground — 5 μm/pass then sliding 10 times	3.1	3.8	3.3	3.6
Annealed	0%	0%	0%	0%
Average grain size as-sintered (μm)	0.41	0.40	0.47	0.40
Average grain size annealed (μm)	0.20	0.17	0.23	0.18

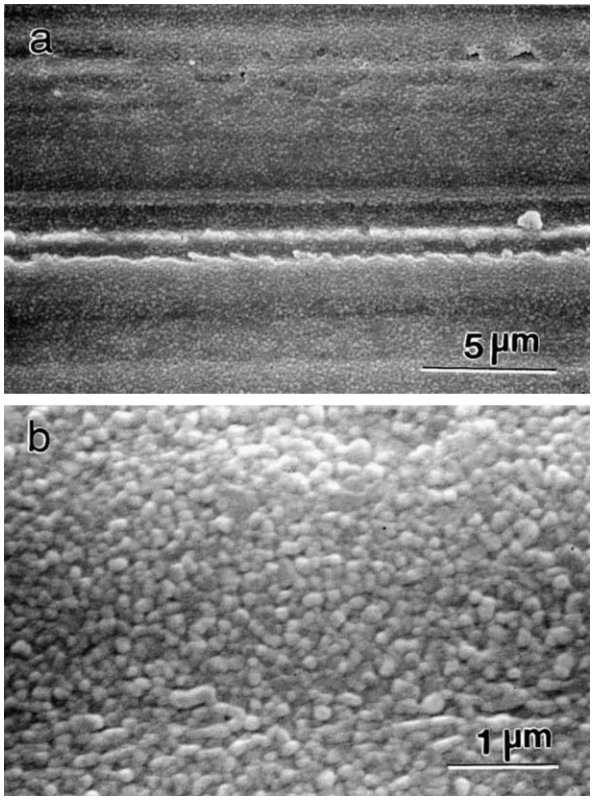

Fig. 7. (a) lower and (b) high magnification of the ground and annealed Tosoh TZYS.

5. Conclusion

The densities, micro structures, Y_2O_3 content and phase transformation of 3 mol% yttria-doped TZPs were investigated. We use the statistical inference to help evaluate the variation of Y_2O_3 content. The conclusions of this research are as follows:

1. The sintered density of four TZPs samples is high which is in the range of 98.5%–99.8% except the PL-D sample. The average grain size of all TZPs is in the range of 0.40–0.47 μm. Sample Tosoh TZYS has the highest sintered density (99.8%) and smaller grain size (0.41 μm). It can be attributed to easy dispersion, free agglomerate, well compaction in green stage and good sinterability. Moreover, Tosoh TZYS sample has the least amounts of large grains ($<0.1\%$) compared to other four TZPs. The grain size decreases from 0.41 to 0.20 μm after surface grinding and heat treatment.

2. The amount of Y_2O_3 content of all TZPs is in the range of 5.00–5.38 mass%, corresponding to 2.80–3.01 mol%. The large grains in the vicinity of residual pores have a lower Y_2O_3 content and the most worst case is found in the sample PL-D and CH9910-Y. That implies the formation of large grains has the relation to a lower Y_2O_3 content.

3. The measurements of Y_2O_3 content quantified either by EDS or WDS are fairly consistent. Tosoh TZYS sample has the best homogeneity of Y_2O_3 content analyzed by SEM-EDS and EPMA. Moreover, it can be found that the samples Tosoh TZYS, Daiichi HSY-3.0 and HWA-ZY3P have similar level of homogeneity of Y_2O_3 content, while the samples PL-D and CH9910-Y show a relatively poor distribution.

4. If a level of homogeneity of $\leqslant \pm 1.0\%$ is desired, several measurement parameters have to be considered, including sample preparation, calibration procedures, accumulated time, and intensity etc. for precise measurement of Y_2O_3 content.

5. From the results obtained by EDS or WDS, both these two techniques provide reliable data. However, WDS measurement is a time-consuming task due to longer collection time compared with EDS.

6. For small sampling if the number of measurement is less than 4, the value of Student's t distribution, $t_{n-1}^{\alpha/2}$ will deviate largely from the real situation. In other words, under the things being equal the confidence coefficient will become too low. Therefore, the number of measurement of Y_2O_3 content for small sample (<30) is suggested to be at least 4 during the quantitative analysis.

7. The grinding by diamond wheel (800 mesh) affects the crystallinity and microstructures of TZP surface. The machining induces t-to-m phase transformation and asymmetrical broadening of (111) peak. The amount of m-phase can increase to 3.1–3.8% after grinding and then decrease to 0% through heat treatment. Besides, the grain size refinement can be achieved through an appropriate heat treatment.

Acknowledgements

The authors would like to thank the National Science Council for the financial support under the contract number NSC87-2622-E-002-014.

References

1. Hannink, R. H. and Swain, M. V., Progress in transformation toughening of ceramics. *Ann. Rev. Mater. Sci.,* 1994, **24**, 359–408.
2. Heuer, A. H., Transformation toughening in ZrO_2-containing ceramics. *J. Am. Ceram. Soc.,* 1987, **70**(10), 689–698.
3. Subbarao, E. C. Zirconia — an overview. In *Advances in Ceramics*, Vol. 3, *Science and Technology of Zirconia,* ed. A. H. Heuer and L. W. Hobbs, 1981, pp. 1–24.
4. Lange, F. F., Transformation toughening Part III: experimental observations in the ZrO_2–Y_2O_3 system. *J. Mater. Sci.,* 1982, **17**, 240–246.
5. Masaki, T., Mechanical properties of toughened ZrO_2–Y_2O_3 ceramics. *J. Am. Ceram. Soc.,* 1986, **69**(8), 638–640.
6. Ho, F. Y., Master thesis, National Taiwan University, 1998.
7. Medelson, M. I., Average grain size in polycrystalline ceramics. *J. Am. Ceram. Soc.,* 1969, **52**, 443–446.
8. *Phoenix User's Manual, SEM quant. ZAF.* EDAX, USA, 1998.
9. *Jeol User's Manual, XM-86PACZAF*, Jeol, Japan.
10. Toraya, H., Yoshimura, M. and Somiya, S., Calibration curve for quantitative analysis of the monoclinic-tetragonal ZrO_2 system by X-ray diffraction. *J. Am. Ceram. Soc.,* 1984, **67**(6), C–119–C-121.
11. Garvie, R. and Nicholson, P. S., Phase analysis in Zirconia system. *J. Am. Ceram. Soc.,* 1972, **55**(6), 303–305.
12. Mendenhall, W., *Introduction to Probability and Statistics.* Duxbury Press, Boston, USA, 1987, Chapter 3, pp. 27–76.
13. Walpole, R. E., *Introduction to Statistics*, 2nd edn. Macmillan, New York, USA, 1974, Chapter 7, pp. 121–152.
14. Chao, L. L. *Introduction to Statistics.* Brooks/Cole, California, USA, 1980, Chapter 3, pp. 48–85.
15. Friedman, H., *Introduction to Statistics.* Random House, New York, USA, 1972, Chapter 7, pp. 91–107.
16. Yakowitz, H., Vieth, D-L., Heinrich, K. F. J. and Michaelis, R. E. *National Bureau of Standards Spec. Pub.*, pp. 260–210, 1965.
17. Goldstein, J. I., Newbury, D. E., Echlin, P., Joy, D. C., Fiori, C. and Lifshin, E., *Scanning Electron Microscopy and X-ray Microanalysis.* Plenum Press, New York, USA, 1939 Chapter 8, pp. 393–445.
18. Yang, C.-C.T., Master thesis, National Taiwan University, 1999.
19. Lange, F. F., Transformation-toughened ZrO_2: correlations between grain size control and composition in the system ZrO_2-Y_2O_3. *J. Am. Ceram. Soc.,* 1986, **69**(3), 240–242.
20. Whalen, P. J., Reidinger, E. and Antrim, R. F., Prevention of low temperature surface transformation by surface recrystallization in yttria-doped tetragonal zirconia. *J. Am. Ceram. Soc.,* 1989, **72**(2), 319–321.
21. Kim, D. J., Jung, H. J. and Kim, H. J., t→r Phase transformation of tetragonal zirconia alloys by grinding. *J. Mater. Sci. Lett.,* 1995, **14**, 285–288.
22. Hasegawa, H., Rhombohedral phase produced in abraded surfaces of partially stabilized zirconia (PSZ). *J. Mater. Sci. Lett.,* 1983, **2**, 91–93.
23. Lankford, J., Page, R. A. and Rabenberg, L., Deformation mechanisms in yttria-stabilized zirconia. *J. Mater. Sci.,* 1988, **23**, 4144–4156.
24. Virkar, A. V. and Matsumoto, L. K., Ferroelastic domain switching as a toughening mechanism in tetragonal zirconia. *J. Am. Ceram. Soc.,* 1986, **69**(10), C-224–C-226.